Stem Cell Reports
Article

OPEN ACCESS

A Double Fail-Safe Approach to Prevent Tumorigenesis and Select Pancreatic β Cells from Human Embryonic Stem Cells

Mirza Muhammad Fahd Qadir,[1,2] Silvia Álvarez-Cubela,[1] Kinsley Belle,[1] Tamar Sapir,[1] Fanuel Messaggio,[1] Kevin B. Johnson,[1] Oliver Umland,[1] Darrell Hardin,[1] Dagmar Klein,[1] Ingrid Pérez-Álvarez,[3] Fatima Sadiq,[4] Oscar Alcázar,[1] Luca A. Inverardi,[1,5,6] Camillo Ricordi,[1,7,8] Peter Buchwald,[1,9] Christopher A. Fraker,[1,8] Ricardo L. Pastori,[1,6] and Juan Domínguez-Bendala[1,2,7,*]

[1]Diabetes Research Institute, University of Miami Miller School of Medicine, Miami, FL 33136, USA
[2]Department of Cell Biology, University of Miami Miller School of Medicine, Miami, FL, USA
[3]University of California Irvine Medical Center, Orange, CA 92868, USA
[4]Center for Specialized Surgery, Florida Hospital, Orlando, FL 32804, USA
[5]Department of Microbiology & Immunology, University of Miami Miller School of Medicine, Miami, FL, USA
[6]Department of Medicine, Division of Metabolism, Endocrinology and Diabetes, University of Miami Miller School of Medicine, Miami, FL, USA
[7]Department of Surgery, University of Miami Miller School of Medicine, Miami, FL, USA
[8]Department of Biomedical Engineering, University of Miami Miller School of Medicine, Miami, FL, USA
[9]Department of Molecular and Cellular Pharmacology, University of Miami Miller School of Medicine, Miami, FL, USA
*Correspondence: jdominguez2@med.miami.edu
https://doi.org/10.1016/j.stemcr.2019.01.012

SUMMARY

The transplantation of human embryonic stem cell (hESC)-derived insulin-producing β cells for the treatment of diabetes is finally approaching the clinical stage. However, even with state-of-the-art differentiation protocols, a significant percentage of undefined non-endocrine cell types are still generated. Most importantly, there is the potential for carry-over of non-differentiated cell types that may produce teratomas. We sought to modify hESCs so that their differentiated progeny could be selectively devoid of tumorigenic cells and enriched for cells of the desired phenotype (in this case, β cells). Here we report the generation of a modified hESC line harboring two suicide gene cassettes, whose expression results in cell death in the presence of specific pro-drugs. We show the efficacy of this system at enriching for β cells and eliminating tumorigenic ones both *in vitro* and *in vivo*. Our approach is innovative inasmuch as it allows for the preservation of the desired cells while eliminating those with the potential to develop teratomas.

INTRODUCTION

Clinical trials have already been initiated for the treatment of type 1 diabetes with hESC-derived β cell progenitors (Schulz et al., 2012), and newer approaches with functional β-like cells are lining up (Pagliuca et al., 2014; Rezania et al., 2014). However, for all their promise, hESCs are not without limitations. While the proportion of β-like cells obtained is relatively high (30%–40%) (Pagliuca et al., 2014; Rezania et al., 2014), a significant percentage of undefined cell types are also generated (Dominguez-Bendala et al., 2016; Pagliuca et al., 2014). Most importantly, non-differentiated escapees may produce teratomas upon transplantation (Kroon et al., 2008). Although recent protocol refinements have reduced this risk, the foreseeable implementation of hESC-based therapies in thousands of patients calls for caution. One single case of hESC-derived tumors may set the field back for years.

To address these concerns, we set out to engineer hESC lines with control mechanisms allowing for the selective ablation of both tumorigenic cells and cells differentiated along undesirable fates. We hypothesized that constructs of our invention would impart such selectivity when stably integrated within the host genome. Given its clinical immediacy, we decided to focus on an insulin-producing cell differentiation model, even though our system could be customized for any cell type. In such a model, cells are engineered with two suicide gene cassettes. One of them (herpes simplex virus thymidine kinase, or HSV-TK) is activated only in cells that resume/continue tumorigenic proliferation. The second (nitroreductase [NTR]) is active in all cells unless they express insulin, in which case it is permanently excised out of the genome. HSV-TK and NTR impart sensitivity to ganciclovir (GCV) (Fareed and Moolten, 2002) and CB1954 (Grove et al., 1999), respectively, which have been tested clinically (Searle et al., 2004; Williams et al., 2015). In our design, the NTR cassette, flanked by *loxP* sites, is eliminated upon expression of Cre by the human insulin promoter (Kuhn and Torres, 2002). Therefore, insulin-expressing cells are rendered insensitive to CB1954. HSV-TK is driven by the telomerase promoter, which is active only in undifferentiated cell types (Albanell et al., 1999). This makes proliferating cells sensitive to GCV. Thus, our method provides a double fail-safe control such that (1) only insulin$^+$, non-proliferating cells survive selection; (2) cells that may de-differentiate after transplantation (Fujikawa et al., 2005) (and in which NTR was lost with the onset of insulin expression) may still be selectively killed *in vivo* by GCV, leaving the rest of the graft intact; and (3) undifferentiated cells are sensitive to two pro-drugs,

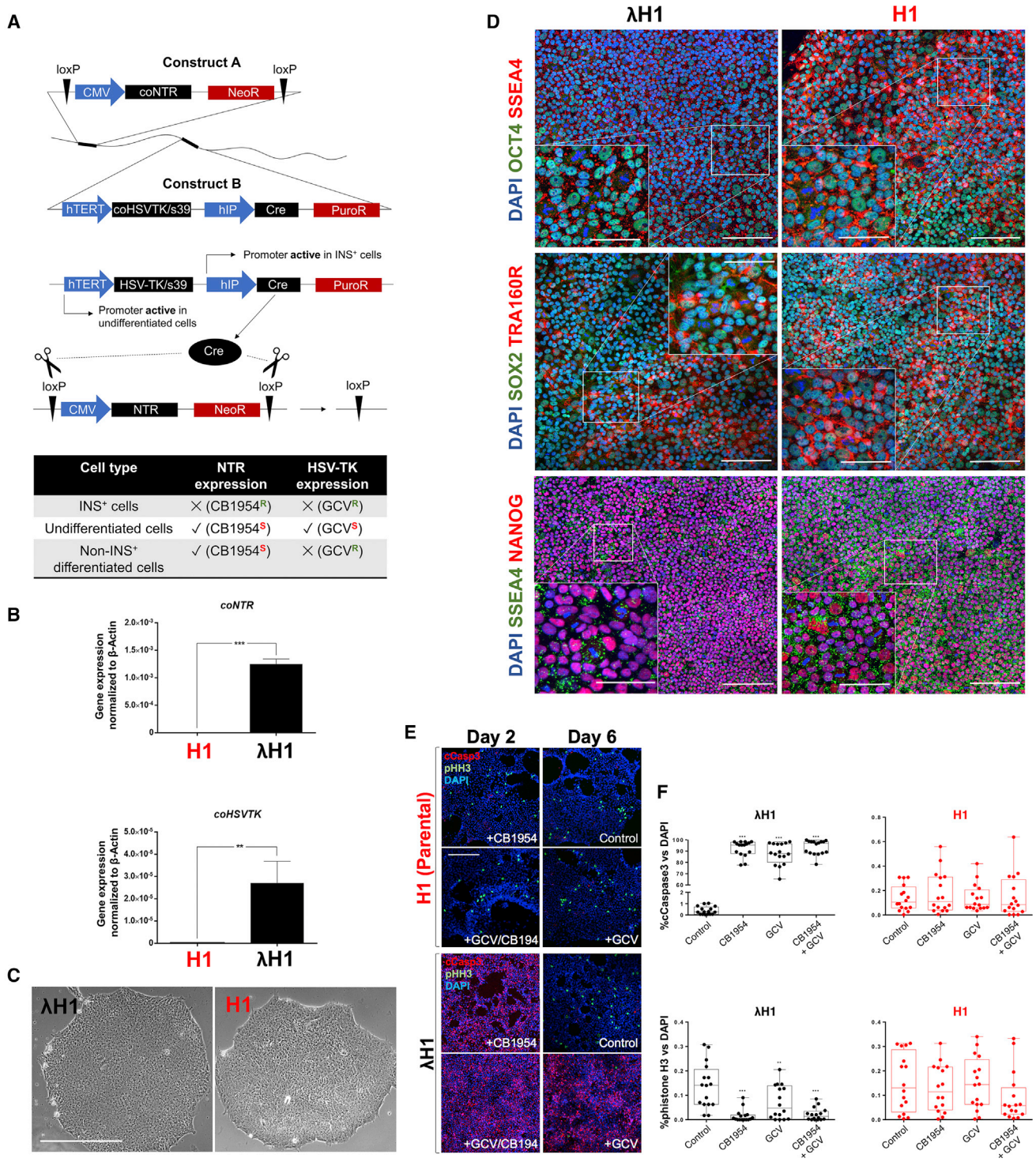

Figure 1. Genetically Modified *λH1* Cells Are Sensitive to the Pro-drugs Ganciclovir (GCV) and CB1954

(A) The structure of construct A comprises: (1) a constitutive cytomegalovirus promoter-enhancer hybrid (CMV)-driven codon optimized (co) nitroreductase gene (NTR); (2) a neomycin resistance gene (NeoR); and (3) *LoxP* sites flanking the above two cassettes in their entirety. Construct B consists of: (1) a human telomerase reverse transcriptase promoter (hTERT)-driven codon optimized (co) herpes simplex virus thymidine kinase S39 mutant gene (HSV-TK/s39); (2) a human insulin promoter (hIP)-driven codon optimized Cre-recombinase gene (Cre); and (3) a puromycin resistance cassette. When the insulin promoter is active, Cre recombinase is produced, and

(legend continued on next page)

making it less likely for tumorigenic cells to survive in case one single drug was insufficient to destroy 100% of them, or if they became resistant to one pro-drug due to spontaneous mutations of the relevant suicide gene (Kotini et al., 2016). No other method reported thus far offers the same degree of safety and specificity, as conventional suicide gene-based strategies bring about the destruction of the entire graft or do not enrich for the cells of therapeutic interest. Our results offer proof-of-principle of this approach and open the door to the subsequent targeting of these constructs to specific "safe harbor" locations within the genome of clinical-grade hESCs.

RESULTS

Suicide Cassette Construction

DNA was synthesized by GenScript (Piscataway, NJ). Owing to the size of both suicide cassettes, we generated two constructs that could be independently transfected. Figure 1A shows the composition of constructs A (*loxP*-CMV-NTR-*loxP*) and B (hTERTP-HSV-TK-hiP-Cre), as well as their predicted function. The main elements of construct A are: (1) *loxP* sites flanking a region that is excised by Cre (Nagy, 2000). (2) Nitroreductase (NTR, T41L/N71S mutant). NTR is a flavoenzyme homodimer with flavin mononucleotide (FMN) cofactors, encoded by the *E. coli nsfB/nfnB* gene (Searle et al., 2004). CB1954 [5-(aziridin-1-yl)-2,4-dinitrobenzamide] is reduced by the FMN to a 4-hydroxylamino derivative, which becomes a cytotoxic DNA crosslinking agent (Grove et al., 1999). Since virus-mediated expression of NTR in tumor cells sensitizes them to CB1954, this strategy has been tested clinically for several types of cancer (Searle et al., 2004; Williams et al., 2015). The double mutant T41L/N71S sensitizes cells to CB1954 concentrations up to ~15-fold lower than the native enzyme (Jaberipour et al., 2010). In our construct, the T41L/N71S NTR gene is driven by the CMV promoter. This plasmid is selectable in neomycin/G418. Upon Cre expression, both NTR and neomycin resistance cassettes are eliminated (Figure 1A).

The main elements of construct B are: (1) HSV thymidine kinase (HSV-TKSR39 mutant). Ganciclovir (GCV) phosphorylation by HSV-TK results in the accumulation of toxic metabolites and cell death (Schipper et al., 2007). As with NTR, this system has been safely tested for the treatment of cancer (Karjoo et al., 2016; Klatzmann et al., 1998). Our construct features an enhanced mutant, HSV-TKSR39 (Black et al., 2001), which also has higher activity at lower doses of the pro-drug (Qasim et al., 2002). This gene is driven by the human telomerase reverse transcriptase (hTERT) promoter. Somatic cells express hTERT at very low levels or not at all, whereas hESCs and most tumoral cells exhibit high levels of expression. As teratomas have high telomerase activity (Albanell et al., 1999), the placement of HSV-TK under the control of the telomerase promoter will lead to the selective expression of the suicide gene in undifferentiated hESCs. (2) Cre is a site-specific bacteriophage recombinase (see *loxP* above) (Nagy, 2000). In our design, Cre will excise out the sequence comprised between the *loxP* sites (NTR cassette). Since Cre is driven by the human insulin promoter (Odagiri et al., 1996), these elements will be eliminated only in cells that express insulin upon differentiation, rendering them insensitive to CB1954 (Figure 1A).

Construct B is selectable in puromycin. Backbone sequences for both constructs feature all bacterial replication and expansion elements. We added Kozak sequences (Kozak, 1987) wherever needed to ensure maximal expression in human cells. Terminators and enhancers were also placed as required for each expression unit. We applied human codon usage optimization during the synthesis of each construct, as some of the mutant sequences contain codons that are used infrequently in highly expressed human genes. Figure S1 shows nucleotide and amino acid sequences of both constructs.

the main elements of construct A (including the NTR cassette) are excised out. As shown in the table, insulin$^+$ cells (INS$^+$) resulting from the differentiation of *λH1* cells are therefore resistant (R) to GCV (since hTERT is not expressed in differentiated cells) and CB1954 (owing to the Cre-mediated excision). In contrast, HSV-TK/s39 and NTR are expressed in undifferentiated cells, which makes them sensitive (S) to both GCV and CB1954. Finally, *λH1* cells differentiated into non-insulin$^+$ cells are resistant to GCV but sensitive to CB1954, since the NTR cassette remains intact.

(B and C) (B) Expression of NTR and HSV-TK genes in modified hESCs as determined by qRT-PCR versus β-actin/18S. Asterisks denote statistical significance: $^{**}p < 0.01$, $^{***}p < 0.001$. (C) Photomicrographs of modified hESCs (*λH1*) and unmodified hESCs (H1) colonies after 6 passages and 8 days of culture on hESC-grade Matrigel-coated culture plates.

(D) Both *λH1* and H1 hESCs express the pluripotency markers OCT4 (green), SSEA4 (red), SOX2 (green), TRA-1-60R (red), SSEA4 (green), and NANOG (red). DAPI (blue) is used as nuclear counterstaining. Insets show higher-magnification details of the cultures.

(E) Phospho-histone H3 (green) and cleaved caspase-3 (red) IF of H1 (top panel) and *λH1* (bottom panel) after treatment (clockwise, from top left) with CB1954, vehicle (control), GCV, and GCV + CB1954. Days 2 and 6 are shown.

(F) Percentages of cleaved caspase-3$^+$ versus DAPI (top) and of phospho-histone H3 versus DAPI (bottom) for both *λH1* and H1 cells following the above treatments (n = 6 independent experiments).

Size bars, 100 μm in (D) and (E), 30 μm insets in (D). A confocal microscope was used for the acquisition of all the images.

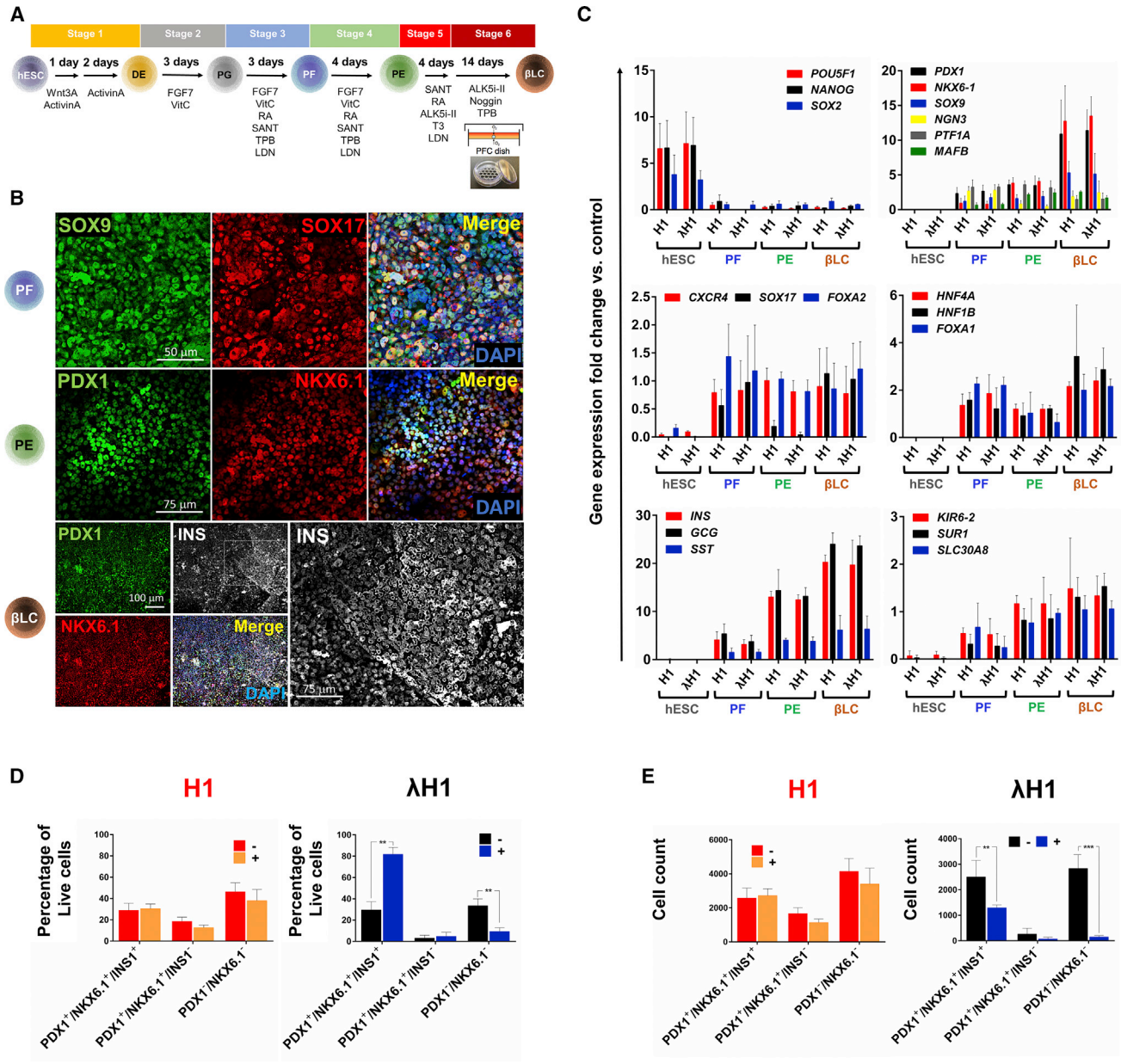

Figure 2. Suicide Cassettes Inserted into *λH1* Cells Function as Predicted upon β-like Cell Differentiation

(A) Differentiation stages for the protocol used to derive β-like cells from *λH1* and H1-hESCs: definitive endoderm (DE), primitive gut (PG), posterior foregut (PF), pancreatic endoderm/pancreatic endocrine precursors (PE), and β-like cells (βLC). A final stage (stage 6, 14 days) involves culturing cell aggregates in an oxygen-permeable perfluorocarbon (PFC)-based AirHive dish, which increases the efficiency of differentiation of mono-hormonal and functional β-like cells from endocrine precursors (PE). For the *in vitro* evaluation of pro-drug-mediated enrichment, GCV (100 μM) and CB1954 (10 μM) were used through the last 7 days of stage 6. The total duration for culture from hESCs to stage 6 is 31 days.

(B) Representative immunofluorescence staining of *λH1* cells throughout the differentiation protocol, showing expression of SOX9 and SOX17 at the PF stage (stage 3, D9); PDX1 (green) and NKX6.1 (red) at the pancreatic endoderm and pancreatic endocrine precursor (PE) stage (stage 4, D13); and PDX1 (green), NKX6.1 (red), and INS (gray) staining at the β-like cell (βLC) stage (stage 5, D17). A higher magnification is shown of an INS^+ region delineated by a dotted box. Nuclear counterstaining: DAPI.

(C) Gene expression profiles of *λH1*- and H1-derived stage 0 (hESC, D0), stage 3 (PF, D9), stage 4 (PE, D13), and stage 5 (βLC, D17) cells. Expression is calculated against neonatal foreskin fibroblasts (NUFFs) after normalization of each marker against 18S-rRNA and β-actin.

(legend continued on next page)

Modified hESCs Express the Transgenes and Maintain Pluripotency

Clones of the hESC line H1 containing both electroporated constructs were selected using puromycin (for A) and neomycin (for B). Twenty-six double-resistant clones were handpicked, expanded under antibiotic selection and cryopreserved. Genomic PCR to confirm integration of both constructs and qRT-PCR to determine which clones had higher transgene expression was performed (Figures S2A–S2D). Based on the results of these assays, clone A (*λH1* from now on) was selected for further testing. As shown in Figure 1B, *λH1* cells express NTR and HSV-TK transgenes. Expression was stable throughout 23 passages post-transfection (Figure S2E). The morphology of *λH1* colonies (Figure 1C) and their pattern of expression of pluripotency markers (as determined by flow cytometry [Figures S3A and S3C], qRT-PCR [Figure S3B], and immunofluorescence [Figure 1D]) were indistinguishable from those observed in the parental (unmodified) H1 cell line. Karyotype analyses before and after the modification showed no abnormalities induced by transgene insertion (data not shown).

λH1 Cells Are Sensitive to Both GCV and CB1954 *In Vitro*

Kill curves using different dosages for GCV (0.01–1,000 μM) and CB1954 (0.1–300 μM) were performed for *λH1* and the parental line. Cell death was quantified by MTT [3-(4,5-dimethylthiazol-2-yl)-2,5-diphenyltetrazolium bromide] assays, which helped us determine optimal pro-drug concentration leading to ablation of undifferentiated *λH1* cells within 7 days, while preserving the parental line viability. Such concentration was between 10 and 100 μM for both GCV and CB1954 (Figure S4A), as reported for other cell types (Felmer and Clark, 2004; Schuldiner et al., 2003). We used 10 μM for CB1954 and 100 μM of GCV for all subsequent experiments. Figure S4B presents the viability curve of both *λH1* and H1 cells when exposed to the above pro-drug dosages for 7 days. Figure 1E presents immunofluorescence (IF) expression of phosphohistone H3 (proliferation)/cleaved caspase-3 (apoptosis) in parental H1 cells (top panel) and *λH1* (bottom panel) after treatment with CB1954, GCV, or a combination of both. Controls received just vehicle. As shown there, and in Figure S4D, the parental H1 line is largely insensitive to either pro-drug, while most *λH1* cells die after just 2 days of exposure to CB1954 and 6 days of exposure to GCV (Figure 1F).

λH1 Cells Differentiate along the β Cell Lineage

Next, we proceeded to differentiate both *λH1* and its parental cell line into β-like cells (Figures 2A–2C) (see Experimental Procedures). Gene expression profiles show no statistical differences between *λH1* and H1 cells at any stage (Figure 2C). The percentage of the pancreatic progenitor markers PDX1$^+$ and NKX6.1$^+$ at the end of stage 4 (PE) (Rezania et al., 2013) was similar for both modified and parental lines (46.4% versus 47.6%, respectively), and aligned with earlier reports (Pagliuca et al., 2014; Rezania et al., 2014; Russ et al., 2015) (Figure S4C).

Suicide Constructs Function as Predicted after β Cell Differentiation *In Vitro*

Once differentiation was completed, we treated both lines with CB1954 and GCV for an additional 7 days and analyzed the resulting populations by flow cytometry (n = 3 independent experiments). Controls were kept in the same conditions, untreated, for the same length of time. As shown in Figure 2D (right panel), the percentage of live *λH1* cells that co-express PDX1$^+$/NKX6.1$^+$/INS$^+$ (a widely accepted β cell signature [Pagliuca et al., 2014; Rezania et al., 2014; Russ et al., 2015]) differs significantly between the untreated (29.6% ± 7.5%) and treated (81.7% ± 6.4%) groups ($p = 0.004$). There was no statistically significant difference in the percentage of PDX1$^+$/NKX6.1$^+$/INS$^-$ cells (likely pancreatic progenitors) between treated and untreated groups. This indicates that these progenitors may already express insulin mRNA at a level high enough to elicit Cre-mediated excision of NTR. In contrast, there was a highly significant ($p = 0.008$) decrease in the percentage of PDX1$^-$/NKX6.1$^-$ cells upon treatment. As for the parental line, there were no statistically significant differences between treated and untreated groups in any of the populations examined (Figure 2D, left panel). Despite the increase in their relative percentage, addition of the pro-drugs resulted in a net decrease in β cell number (Figure 2E, right panel), probably due to bystander ("kiss of death") effect (Andrade-Rozental et al., 2000).

To discard the possibility that the pro-drugs may negatively affect the phenotype of the selected β-like cells, we conducted qRT-PCR of key pancreatic endocrine genes for

(D) Fluorescence-activated cell sorting (FACS) analysis (percentage of live cells) for PDX1, NKX6.1, and INS in *λH1*- and H1 cell-derived stage 6 cells after treatment (+) with the pro-drugs GCV (100 μM) and CB1954 (10 μM). Untreated controls (0.043% DMSO) (−) are also shown for comparison.

(E) FACS analysis (total cell count) for PDX1, NKX6.1, and INS, in λH1- and H1-hESC-derived stage 6 cells after treatment (+) or untreated (−) control.

Error bars: standard error. ***$p < 0.001$, **$p < 0.01$, *$p < 0.05$. n = 6 independent experiments. Images were acquired with an inverted fluorescence microscope.

both treated and untreated *λH1* and H1 cells (Figure 3A). As expected, neither the parental line nor untreated *λH1* showed significant differences. In contrast, the expression of several genes involved in insulin secretion was significantly upregulated in the *λH1* cells that received both pro-drugs versus the untreated ones. This suggests that, far from exerting a deleterious effect on the function of β cells, selection and enrichment by the pro-drugs may in fact improve it. Perifused non-treated, differentiated *λH1* cells exhibited a glucose-responsive insulin secretion pattern similar to that of differentiated H1 (Figure 3B, left panel). In contrast, *λH1* cells selected with GCV and CB1954 exhibit a stronger (normalized by DNA content) response than the parental line (Figure 3B, right panel), in all likelihood reflecting the corresponding enrichment in β cells. The perifusion response of four human islet preparations is shown for comparison in Figure S6. Additional measurements of C-peptide at low and high glucose (Figure 3C) and total insulin/C-peptide (Figure 3D), further confirm enhanced responses in the treated versus untreated *λH1* groups.

Also, as predicted, *λH1* cells (clone A) had nearly undetectable expression of both transgenes at the β cell stage (Figure 3E). For HSV-TK, this is due to lack of expression of hTERT in β cells, but not to loss of the transgene (Figure S5C). For NTR, in contrast, lack of expression is due to loss of the transgene following Cre-mediated recombination (Figure S5C).

Treatment with Either GCV or CB1954 Prevents the Formation of and Eliminates Fully Formed Teratomas in Immunodeficient Mice Xenotransplanted with λH1 Cells

To test whether our strategy worked as intended *in vivo*, 5×10^6 undifferentiated *λH1* cells were transplanted subcutaneously into 5–6-week-old immunodeficient NOD-SCID (non-obese diabetic-severe combined immunodeficiency) mice. Groups were assigned as follows: control (vehicle treatment, n = 3; Figure 4A); peri-transplantation treatment with GCV (40 mg/kg; 5 days, starting the seventh day after transplantation, n = 4; Figure 4B); and peri-transplantation treatment with CB1954 (20 mg/kg; 5 days, starting the seventh day after transplantation, n = 4; Figure 4C). Tumors could be palpated and measured using calipers in the control group starting at week 6–7 (Figure 4A). At week 10, one of the mice was euthanized for histopathological characterization of the teratoma, which expectedly showed derivatives of the three germ layers (Figure 4A). Starting on week 11, we treated the remaining two mice with GCV and CB1954 to test whether pro-drug administration would eliminate already formed tumors. Indeed, tumor volume receded to undetectable levels within 3 weeks (Figure 4A).

No tumors could be detected in the GCV-pretreated group up to week 10, 4 weeks after tumors were first detected in the control group. Two mice were euthanized at this point, showing no tumors (data not shown). However, examination of the remaining two animals suggested the presence of small teratomas, so we observed them for an additional week. During this period, the tumors grew significantly. This could be due to either the carry-over of residual hESC escapees that survived the initial GCV regimen, or to the development of GCV-resistant mutations in HSV-TK, as described previously (Kotini et al., 2016). To test these two hypotheses, we re-treated these animals with GCV in a 5-day drug/2-day rest regimen for the following 3 weeks. The complete disappearance of both tumors (Figure 4B), as determined both by manual palpation and necropsy after euthanasia, confirmed the former hypothesis. Finally, none of the animals in the third group (treated in the peri-transplantation period with CB1954) developed tumors (Figure 4C).

To determine whether pro-drug treatment affected functionality *in vivo,* we transplanted an additional 12 NOD-SCID mice with fully differentiated cells. Four mice were transplanted with 1×10^6 differentiated H1 cells (control group) and 8 with the same number of *λH1* cells (Figure 5A). Out of these, four received GCV + CB1954 pre-selected *λH1* cells. The remaining four were transplanted with non-selected *λH1* cells and treated with the two pro-drugs 3 weeks after transplantation (dosage/regimen as above) (see Figure 5B for research scheme). Basal circulating human C-peptide was determined just prior to transplantation and at weeks 2, 4, 6, and 8 for each group. Figure 5C shows that the secretion of human C-peptide, as previously reported, follows a similar uptrend with time for all groups as they further mature *in vivo* (Rezania et al., 2014). Functionality was affected neither by the genetic modification nor by the subsequent selection with the pro-drugs *in vivo*, as demonstrated by glucose-stimulated C-peptide release assays at weeks 6 and 8 (Figure 5D). At the last time point examined prior to euthanasia (week 8), there were no statistically significant differences between the three groups in human C-peptide secretion or glucose-stimulated C-peptide release. Analysis of the grafts after euthanasia revealed abundant teratoma-like lesions and OCT4 signal in the subcapsular space of mice transplanted with H1 cells (Figure 5E, top and inset). However, none of the animals transplanted with *λH1* cells (whether selected *in vitro* or *in vivo*) exhibited such tumorigenic features (H&E staining of grafts following *in vitro* selection shown as an example, Figure 5E, bottom). Insulin- and PDX1-positive clusters were comparable in all groups, although they were more dispersed and represented a smaller proportion of the overall graft in the H1 group. Glucagon IF signal was low in the H1

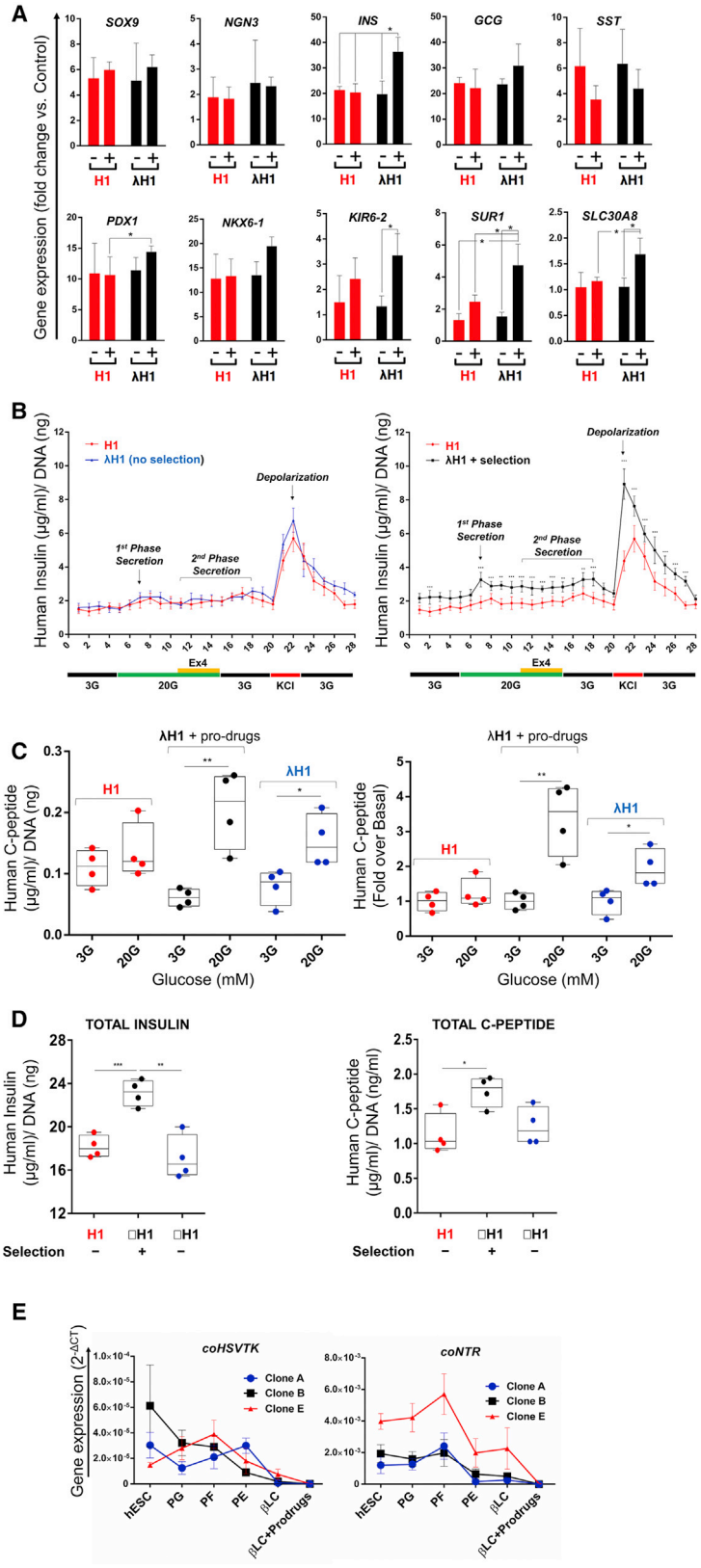

Figure 3. Modified Cells Have Intact β-like Cell Functionality upon Differentiation

(A) Gene expression profiles of select genes for *λH1*- and H1 cell-derived stage 6 (βLC, D31) cells that were either treated (+) with GCV (100 μM) and CB1954 (10 μM) or untreated (−) (control, 0.043% DMSO). Expression is calculated against NUFFs after normalization of each marker against 18S-rRNA and β-actin. n = 6 independent experiments.

(B) Left, dynamic perifusion analysis of H1-differentiated (red line) and *λH1*-differentiated (blue line) cells (no selection). The x axis shows time points of supernatant collection as well as the glucose concentrations used: 3G (3 mM, low) and 20G (20 mM, high). KCl is used to depolarize the membrane and release accumulated insulin. Exendin-4 (Ex-4) is used to stimulate the second-phase secretion. y axis: human insulin (μg/mL)/DNA (ng). Right, dynamic perifusion analysis of H1 cells (red line) and *λH1* cells after pro-drug selection (black line). Asterisks denote statistically significant differences at any given data point: **p < 0.01, ***p < 0.001.

(C) Glucose-stimulated human C-peptide release for H1 cells (red) and selected (black) or unselected (blue) cells, expressed in μg/mL/DNA (ng) (left) or fold increase over basal (right). Asterisks denote statistically significant differences at any given data point: *p < 0.05; **p < 0.01.

(D) Total insulin (left) and C-peptide (right) of H1 cells (red) and selected (black) or unselected (blue) cells, expressed in μg/mL/DNA (ng). Asterisks denote statistically significant differences at any given data point: *p < 0.05, **p < 0.01, ***p < 0.001.

(E) mRNA gene expression profiles of *coHSVTK* and *coNTR* at different stages of differentiation and after treatment with pro-drugs (n = 6 independent experiments). Expression is calculated against NUFF gene expression and normalized against 18s-rRNA and β-actin gene expression. Clone A is *λH1*. Other clones are shown for comparison.

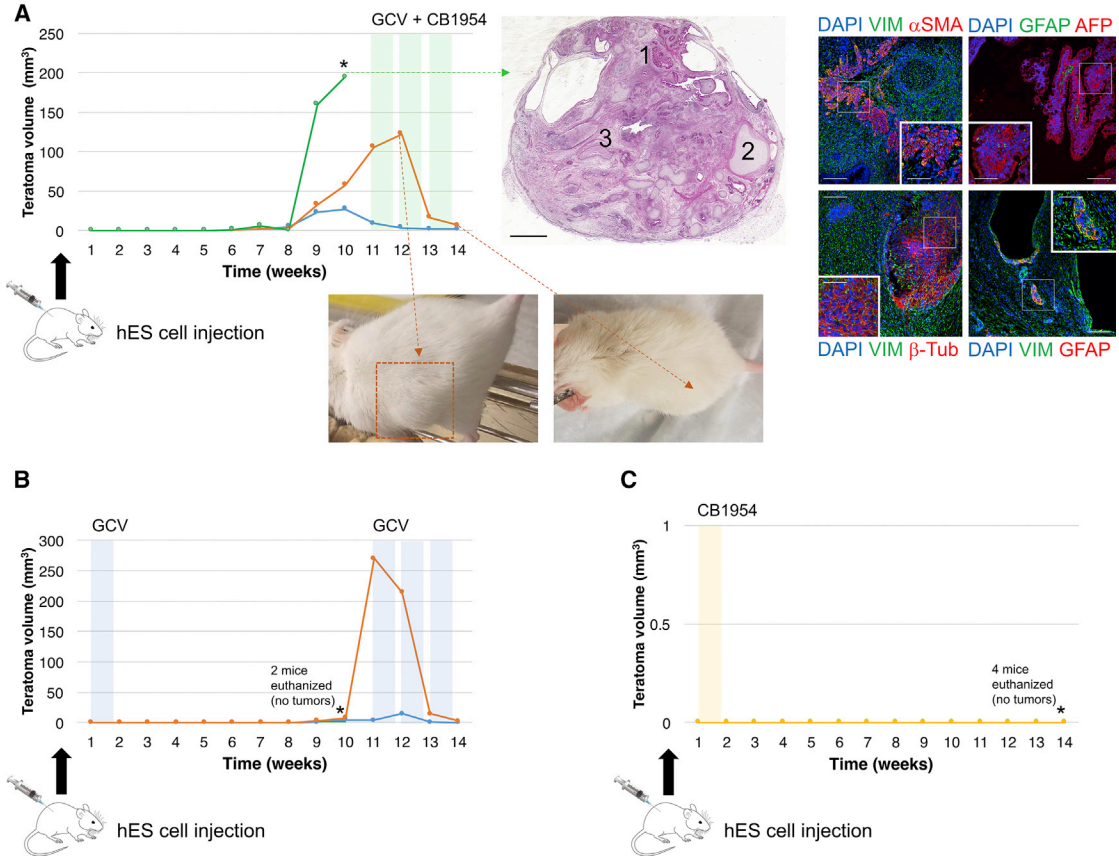

Figure 4. *λH1* Cells Are Sensitive to GCV and CB1954 upon Transplantation in Mice

(A) Progression of tumor (teratoma) volume with time in mice transplanted with *λH1* cells subcutaneously. At week 10, one mouse was euthanized to confirm tumor formation by histological analysis. *Euthanasia point. The tumor was stained with H&E for the identification of teratoma-associated tissues: (1) mucinous glandular epithelium (endoderm); (2) bone/ossified cartilage (mesoderm); and (3) cartilage (mesoderm). Scale bar, 500 μm. Representative immunofluorescence images of the teratoma (right panel) show positive staining for the three germ layers: mesoderm (αSMA$^+$ region), endoderm (AFP$^+$ region), and ectoderm (β-Tub$^+$ region). Neuroectoderm (GFAP$^+$ region) was also readily detected. Scale bars, 100 μm for main panels and 50 μm for insets. Two mice exhibiting external signs of tumor growth were allowed to progress for another week and then treated at week 11 post-transplantation with GCV and CB1954. Five-day treatments are represented as shaded green colored blocks (spaces represent a 2-day rest between treatments). The tumors disappeared completely by week 14, as judged by external measurements and upon histological analysis after euthanasia. Shown in the picture is the same mouse at week 12 (exhibiting a large subcutaneous growth) and week 14, without any signs of teratoma.

(B) Progression of teratoma volume in a group of mice treated with GCV for 5 days, 1-week post transplantation. Two mice euthanized at week 11 (*) did not have any tumors, as confirmed by histological analysis upon euthanasia. However, two mice developed "escape" tumors, probably due to insufficient GCV-induced killing of undifferentiated cells. However, further GCV treatment (3 weeks, 5-day treatment + 2-day rest, represented by blue shaded blocks) resulted in the total ablation of the tumors.

(C) Progression of teratoma volume in a group of mice treated with CB1954 for 5 days, 1-week post transplantation (beige shaded block). Fourteen weeks post-transplantation, none of the mice had developed teratomas. (A) n = 3 mice; (B and C) n = 4 mice. (A and B) Dosage of GCV: 40 mg/kg of body weight. (A and C) Dosage of CB1954: 20 mg/kg of body weight.

group, but almost non-detectable in the others (Figure 5F). We conducted quantification of insulin and glucagon signal in multiple grafts within each group. As shown in Figure 5G, the number of β-cells/field was higher in *λH1* cell grafts than in those of H1 cells ($p < 0.005$ between *in vitro*-treated *λH1* and H1; $p < 0.01$ between *in vivo*-treated *λH1* and H1). In contrast, and as expected, the number of glucagon-positive cells was significantly higher in H1 than either *in vitro* or *in vivo*-treated *λH1* grafts (Figure 5H). Notably, ~85% of the few surviving α-cells in the *λH1* grafts were found to also co-express insulin (Figure 5H, pie charts), which may explain their selective survival. Polyhormonal cells, albeit rare in current endocrine differentiation protocols, are still routinely detected (Russ et al.,

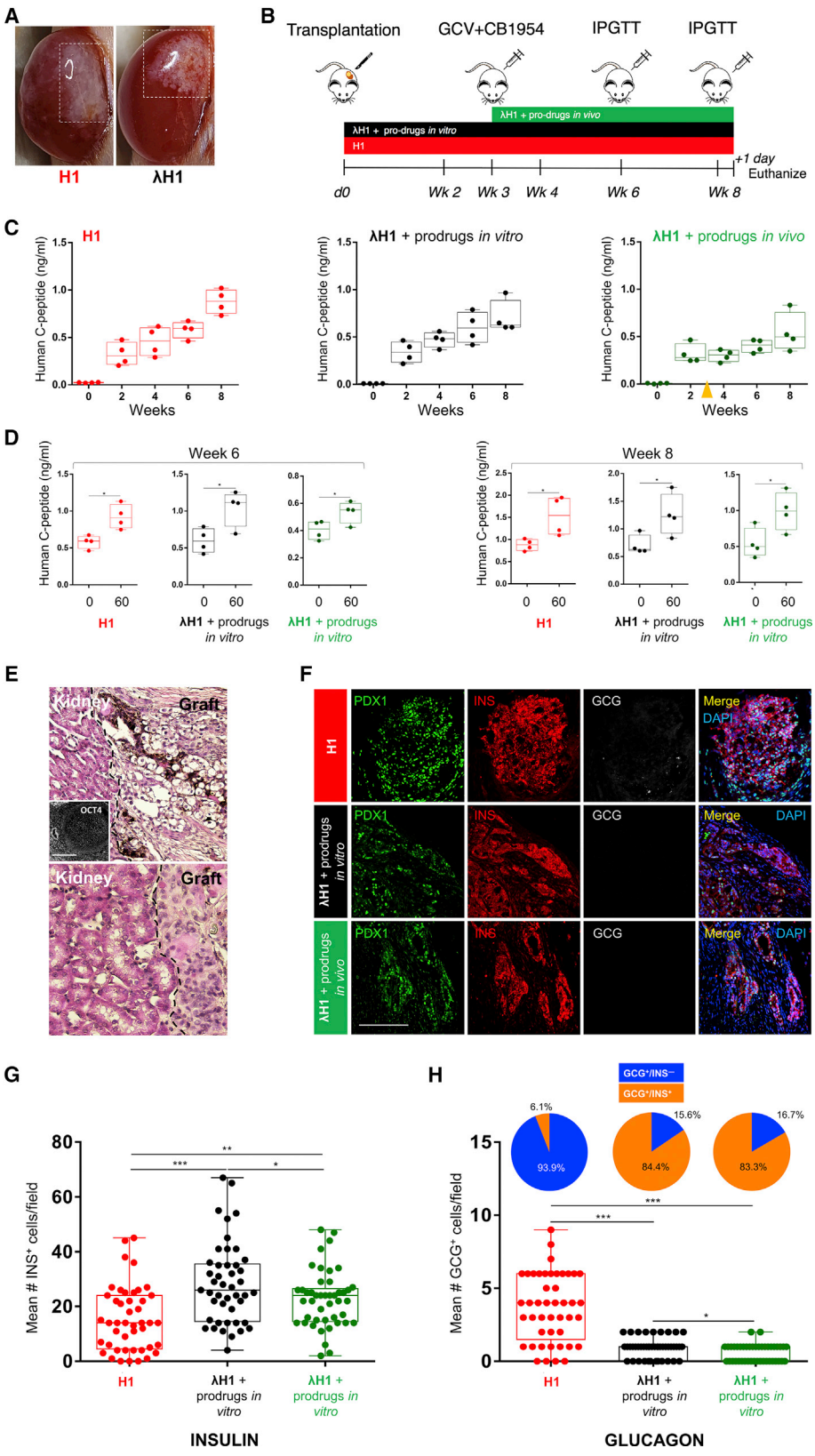

(legend on next page)

2015). Only 6% of the glucagon-expressing cells in the H1 grafts co-expressed insulin (Figure 5H, pie chart).

DISCUSSION

The risk of iatrogenic tumorigenesis has been recognized from very early on in the context of hESC transplantation. While tumors can be treated by standard cytotoxic treatments such as radiotherapy (Marcu et al., 2018) or, more recently, oncolytic viruses (Andtbacka et al., 2015), it stands to reason that regulatory agencies will demand the means to prevent, rather than ablate, hESC-derived teratomas (Fox, 2008).

It has been argued that, if the number of undifferentiated cells/batch is below the threshold known to produce teratomas in immunodeficient mice, these preparations should be safe (Vogel, 2005). However, this does not consider the risk of de-differentiation after transplantation (Fujikawa et al., 2005). hESC-based therapies are predicted to reach millions. It would take only one clinical incidence of tumorigenesis to bring the entire field to a screeching halt, perhaps for years. It is for this reason that others have proposed the use of suicide genes under constitutive promoters (Schuldiner et al., 2003). However, in such a setting, the pro-drug would kill the whole graft, including the cells for which there was a need in the first place. The use of the hTERT promoter driving HSV-TK has been recently described to address this problem (Tian et al., 2013), but such approach by itself does not offer differentiation selectivity. Our method is innovative because it allows for the selective preservation and enrichment of the desired cells while destroying those with tumorigenic potential. The provision of a double fail-safe mechanism is another feature of our system, as tumorigenic escapees would be sensitive to not one but two pro-drugs. This is of special importance following the report of GCV resistance mutations in HSV-TK (Kotini et al., 2016), as any such mutation would compromise the entire approach. To our knowledge, no similar tactic has been described thus far. If successful, our strategy has far-reaching applications beyond diabetes. Selectivity could be adjusted for other settings by simply replacing the insulin promoter by regulatory sequences specific to the cell of interest. Our research is particularly timely in the context of hESC-derived β-like cell transplantation for the treatment of type 1 diabetes, which is now at the clinical trial stage. Owing to shortcomings of the Encaptra immunoisolation device used in their first wave of trials (Henry et al., 2018), Viacyte has recently initiated the transplantation of non-immunoisolated hESC derivatives into immunosuppressed patients (clinicaltrials.gov identifier:

Figure 5. Differentiated *λH1* Cells Are Functional *In Vivo* Regardless of whether Selection Occurs prior to or after Transplantation

(A) A total of 1×10^6 cells (H1, left; *λH1*, right) were transplanted into the kidney capsule of recipient immunodeficient mice. Pictures show the region where the cells were placed in the subcapsular space of the externalized kidney.

(B) Schematic depiction of the experimental plan, indicating groups and treatments.

(C) Circulating human C-peptide (ng/mL) at 0 (baseline), 2, 4, 6, and 8 weeks of NOD-SCID mice transplanted with H1 cells (left), *λH1* cells pre-treated with the pro-drugs prior to transplantation (center), and unselected, differentiated *λH1* cells (right). In the last group, mice received a course of injections of CB154 (20 mg/kg) and GCV (40 mg/kg) at week 3 after transplantation (orange arrow).

(D) *In vivo* glucose-stimulated human C-peptide release assays conducted at weeks 6 (left) and 8 (right) for each one of the groups (H1 cells, *λH1* cells + pro-drugs *in vitro*, and *λH1* cells + pro-drugs *in vivo*). Left columns show basal human C-peptide secretion (time point 0) and right columns following glucose bolus administration (time point 60 min). Asterisks denote statistically significant differences at any given data point: *$p < 0.05$.

(E) H&E staining of the graft region in a representative H1-transplanted mouse (top), showing keratinized cells (ectoderm), and bone (mesoderm) and epithelial cells (endoderm). Inset shows OCT4 staining in another region of the graft. Bottom: H&E staining of a representative mouse transplanted with *λH1* cells pre-treated *in vitro* with the pro-drugs (grafts of *in-vivo*-treated cells have the same appearance). Scale bar, 100 μm.

(F) Representative IF staining of PDX1 (green), insulin (INS) (red) and glucagon (GCG) (light gray) in grafts from H1 cells (top row), *λH1* cells pre-treated with the pro-drugs prior to transplantation (middle row) and *λH1* cells treated with the pro-drugs after transplantation (bottom row). In general, insulin-positive clusters were less dispersed in the last two groups than in H1 grafts. Glucagon signal was virtually undetectable in *λH1* cell-transplanted animals. Scale bar, 100 μm.

(G and H) Absolute quantification of insulin$^+$ cells (mean number of cells/field) (G) and glucagon$^+$ cells (H) in randomly selected regions across kidney grafts for transplanted stage 6 cells in all groups. Multiple sections (every 10 μm) were quantified to ensure maximal graft coverage. Only nucleated (DAPI$^+$) cells were counted. n = 4/group. *$p < 0.05$; **$p < 0.01$; ***$p < 0.005$. The glucagon graphic also shows pie charts with the percentages of bi-hormonal (glucagon$^+$/insulin$^+$) and mono-hormonal (glucagon$^+$) cells within the glucagon$^+$ population, as determined by imaging quantification. The number of glucagon-positive cells was significantly higher in H1 than either *in vitro* or *in vivo*-treated *λH1* grafts. The majority of the few surviving α-cells in the *λH1* grafts were found to also co-express insulin (84.4% and 83.3% for *in vitro* and *in vivo* treated, respectively), which may explain their selective survival. In contrast, >93% of the glucagon$^+$ cells in the H1 grafts were mono-hormonal.

NCT03163511). Therefore, the two safeguards previously featured by the approach (i.e., a physical barrier that prevented cell escape and a fully competent immune system of the host) are now gone.

Here we present evidence that the insertion of a double suicide gene cassette imparts differentiation selectivity and protection against potential tumorigenesis in hESCs. Genetically modified cells can be selected *in vitro* or *in vivo* for the enrichment of insulin-producing cells. This selection has no impact in the overall functionality of the cells, as demonstrated by a battery of tests both *in vitro* and after transplantation. In fact, following selection, modified hESC preparations generally exhibit stronger functional responses than their unmodified and modified/unselected counterparts, probably owing to β-like cell enrichment on a per cell basis.

It is worth mentioning that selection results in some loss of β-like cells, as expected of the bystander or kiss of death effect. In short, toxic metabolites are transmitted from pro-drug-sensitive cells to adjacent pro-drug-resistant cells (Andrade-Rozental et al., 2000). However, considering the high percentage of β-like cells in our protocol (which may have led to a high local concentration of CB1954 toxic by-products), the effect was not as marked as potentially expected. When mice were treated *in vivo* with both pro-drugs 3 weeks after transplantation, at the 4-week time point the overall secretion of human C-peptide was only slightly lower than that measured for parental or *λH1* cells pre-selected prior to transplantation. Despite this temporary stalling, likely reflective of bystander β cell death at that point, the maturation trend remained intact (i.e., human C-peptide secretion kept increasing with time), and at the 8-week time point there were no statistically significant differences in human C-peptide secretion or glucose stimulation index between any of the three groups. Absolute C-peptide values are generally aligned, on a per cell basis, with those described in Rezania et al. (2014), a widely considered standard in hESC-to-β cell differentiation methods.

Our study indicates that teratomas can be largely prevented by treating the recipient of the cells with the pro-drugs in the peri-transplantation period. More importantly, even if some cells were to escape and eventually give rise to full-fledged teratomas, they can be safely ablated by re-administration of the two drugs. *In vivo* treatment still largely preserves β cell mass and function. It has been reported that constitutive Cre expression may be harmful to the cell (Janbandhu et al., 2014), albeit only at high transgene dosages. Prolonged, low levels of Cre activity permit recombination without concomitant toxicity (Loonstra et al., 2001). Our observation that β-like cells differentiated from λH1 cells show no functional impairment compared with their parental-derived counterparts would suggest that, in our setting, there is no meaningful Cre-associated toxicity, at least throughout the 8-week time frame on which we report. Longer-term follow-up studies would be necessary to fully ascertain any potential damage.

Although other suicide gene-based strategies to avoid tumorigenesis have been described in the literature (Hara et al., 2008; Kojima et al., 2018; Tsujimura et al., 2018), none thus far has also provided the means to selectively preserve the cells of interest. The present study is proposed as proof-of-principle for the subsequent generation of clinical-grade hESCs in which the integration of these constructs is targeted to safe genomic harbors, minimizing the risk of insertional mutagenesis (Baum et al., 2006) and ensuring the selection of single-copy integrations. hESC lines modified in this fashion would be considered safe for transplantation.

EXPERIMENTAL PROCEDURES

Cell Culture and MTT Growth Assay

hESCs (H1 clone, p. 75) were cultured as described (Schuldiner et al., 2000) using mTeSR (cat. no. 05,850, STEMCELL Technologies, Vancouver, Canada; https://www.stemcell.com/). Additional methods for plasmid generation, hESC transfection, differentiation and fluorescence-activated cell sorting/immunofluorescence analysis of differentiation outcomes are described in Supplemental Experimental Procedures.

Teratoma Assays

All animal experiments were conducted under the supervision of the University of Miami Institutional Animal Care and Use Committee. NOD-SCID mice (5–6 weeks old; Jackson Laboratory, Bar Harbor, ME, USA, https://www.jax.org) were housed in specific pathogen-free conditions at the Division of Veterinary Resources. Transplantation methods are detailed in Supplemental Experimental Procedures.

Statistics

GraphPad Prism v.5 was used for statistical analysis. Following the Shapiro-Wilk normality test, statistical differences between groups were calculated by two-tailed paired t test or Wilcoxon signed rank test with 95% confidence intervals (*$p < 0.05$, **$p < 0.01$, ***$p < 0.001$). Results are expressed as means ± SD.

SUPPLEMENTAL INFORMATION

Supplemental Information includes Supplemental Experimental Procedures, six figures, and one table and can be found with this article online at https://doi.org/10.1016/j.stemcr.2019.01.012.

AUTHOR CONTRIBUTIONS

M.M.F.Q., S.A.-C., and K.B. designed and performed the experiments along with analysis and interpretation of the data. T.S.,

O.U., O.A., F.M., K.B.J., and D.H. performed experiments and analyzed data. K.B.J., I.P.-A., and F.S. analyzed histological sections. D.K., L.A.I., P.B., C.R., and R.L.P. contributed discussion and advice on experimental design. J.D.-B. conceived and designed the study and compiled the manuscript. M.M.F.Q., S.A.-C., D.K., R.L.P., and J.D.-B. revised the manuscript. The University of Miami, C.R., L.I., and J.D.-B., are stockholders in Ophysio, licensee of the intellectual property used in this study.

ACKNOWLEDGMENTS

In memoriam: *Jim McWhir* (*1952–2017*). We thank P. F. Searle (University of Birmingham, UK) for the sequence of the T41L/N71S NTR mutant, kindly offered to us before its publication. The same gratitude is extended to W. Qasim (UCL, UK) for the sequence of HSV-TKSR39 and R. Felmer (University de la Frontera, Chile) for helpful discussion and advice. We are also grateful to Drs. Diego Correa, Dimitrios Kouroupis, Michael Bellio, as well as to the Flow Cytometry Core and Translational Models Core, both at the Diabetes Research Institute. M.M.F.Q. is supported by a Fulbright pre-doctoral fellowship. This study was funded by the Juvenile Diabetes Research Foundation (JDRF) (grant number 5-2006-392) and the Diabetes Research Institute Foundation (DRIF). We want to specially thank Mr. Harold Doran, the Inserra family, and the Tonkinson Foundation for their generous support of this work through the years. J.D.-B. is the guarantor of this work and, as such, had full access to all the data in the study and takes responsibility for the integrity of the data and the accuracy of the analysis. The University of Miami, C.R., L.I., and J.D.B., are stockholders in Ophysio, licensee of the intellectual property used in this study.

Received: March 8, 2018
Revised: January 16, 2019
Accepted: January 17, 2019
Published: February 14, 2019

REFERENCES

Albanell, J., Bosl, G.J., Reuter, V.E., Engelhardt, M., Franco, S., Moore, M.A., and Dmitrovsky, E. (1999). Telomerase activity in germ cell cancers and mature teratomas. J. Natl. Cancer Inst. *91*, 1321–1326.

Andrade-Rozental, A.F., Rozental, R., Hopperstad, M.G., Wu, J.K., Vrionis, F.D., and Spray, D.C. (2000). Gap junctions: the "kiss of death" and the "kiss of life". Brain Res. Brain Res. Rev. *32*, 308–315.

Andtbacka, R.H., Kaufman, H.L., Collichio, F., Amatruda, T., Senzer, N., Chesney, J., Delman, K.A., Spitler, L.E., Puzanov, I., Agarwala, S.S., et al. (2015). Talimogene laherparepvec improves durable response rate in patients with advanced melanoma. J. Clin. Oncol. *33*, 2780–2788.

Baum, C., Kustikova, O., Modlich, U., Li, Z., and Fehse, B. (2006). Mutagenesis and oncogenesis by chromosomal insertion of gene transfer vectors. Hum. Gene Ther. *17*, 253–263.

Black, M.E., Kokoris, M.S., and Sabo, P. (2001). Herpes simplex virus-1 thymidine kinase mutants created by semi-random sequence mutagenesis improve prodrug-mediated tumor cell killing. Cancer Res. *61*, 3022–3026.

Dominguez-Bendala, J., Lanzoni, G., Klein, D., Alvarez-Cubela, S., and Pastori, R.L. (2016). The human endocrine pancreas: new insights on replacement and regeneration. Trends Endocrinol. Metab. *27*, 153–162.

Fareed, M.U., and Moolten, F.L. (2002). Suicide gene transduction sensitizes murine embryonic and human mesenchymal stem cells to ablation on demand–a fail-safe protection against cellular misbehavior. Gene Ther. *9*, 955–962.

Felmer, R.N., and Clark, J.A. (2004). The gene suicide system Ntr/CB1954 causes ablation of differentiated 3T3L1 adipocytes by apoptosis. Biol. Res. *37*, 449–460.

Fox, J.L. (2008). FDA scrutinizes human stem cell therapies. Nat. Biotechnol. *26*, 598–599.

Fujikawa, T., Oh, S.H., Pi, L., Hatch, H.M., Shupe, T., and Petersen, B.E. (2005). Teratoma formation leads to failure of treatment for type I diabetes using embryonic stem cell-derived insulin-producing cells. Am. J. Pathol. *166*, 1781–1791.

Grove, J.I., Searle, P.F., Weedon, S.J., Green, N.K., McNeish, I.A., and Kerr, D.J. (1999). Virus-directed enzyme prodrug therapy using CB1954. Anticancer Drug Des. *14*, 461–472.

Hara, A., Aoki, H., Taguchi, A., Niwa, M., Yamada, Y., Kunisada, T., and Mori, H. (2008). Neuron-like differentiation and selective ablation of undifferentiated embryonic stem cells containing suicide gene with Oct-4 promoter. Stem Cells Dev. *17*, 619–627.

Henry, R.H., Pettus, J., Wilensky, J., Shapiro, J., Senior, P.A., Roep, B., Wang, R., Kroon, E.J., Scott, M., D'Amour, K., and Foyt, H. (2018). Initial clinical evaluation of VC-01TM combination product—a stem cell-derived islet replacement for type 1 diabetes (T1D). Diabetes *67*(Suppl. 1). https://doi.org/10.2337/db18-138-OR.

Jaberipour, M., Vass, S.O., Guise, C.P., Grove, J.I., Knox, R.J., Hu, L., Hyde, E.I., and Searle, P.F. (2010). Testing double mutants of the enzyme nitroreductase for enhanced cell sensitisation to prodrugs: effects of combining beneficial single mutations. Biochem. Pharmacol. *79*, 102–111.

Janbandhu, V.C., Moik, D., and Fassler, R. (2014). Cre recombinase induces DNA damage and tetraploidy in the absence of loxP sites. Cell Cycle *13*, 462–470.

Karjoo, Z., Chen, X., and Hatefi, A. (2016). Progress and problems with the use of suicide genes for targeted cancer therapy. Adv. Drug Deliv. Rev. *99*, 113–128.

Klatzmann, D., Cherin, P., Bensimon, G., Boyer, O., Coutellier, A., Charlotte, F., Boccaccio, C., Salzmann, J.L., and Herson, S. (1998). A phase I/II dose-escalation study of herpes simplex virus type 1 thymidine kinase "suicide" gene therapy for metastatic melanoma. Study Group on Gene Therapy of Metastatic Melanoma. Hum. Gene Ther. *9*, 2585–2594.

Kojima, K., Miyoshi, H., Nagoshi, N., Kohyama, J., Itakura, G., Kawabata, S., Ozaki, M., Iida, T., Sugai, K., Ito, S., et al. (2018). Selective ablation of tumorigenic cells following human induced pluripotent stem cell-derived neural stem/progenitor cell transplantation in spinal cord injury. Stem Cells Transl. Med. https://doi.org/10.1002/sctm.18-0096.

Kotini, A.G., de Stanchina, E., Themeli, M., Sadelain, M., and Papapetrou, E.P. (2016). Escape mutations, ganciclovir resistance, and

teratoma formation in human iPSCs expressing an HSVtk suicide gene. Mol. Ther. Nucleic Acids *5*, e284.

Kozak, M. (1987). An analysis of 5′-noncoding sequences from 699 vertebrate messenger RNAs. Nucleic Acids Res. *15*, 8125–8148.

Kroon, E., Martinson, L.A., Kadoya, K., Bang, A.G., Kelly, O.G., Eliazer, S., Young, H., Richardson, M., Smart, N.G., Cunningham, J., et al. (2008). Pancreatic endoderm derived from human embryonic stem cells generates glucose-responsive insulin-secreting cells in vivo. Nat. Biotechnol. *26*, 443–452.

Kuhn, R., and Torres, R.M. (2002). Cre/loxP recombination system and gene targeting. Methods Mol. Biol. *180*, 175–204.

Loonstra, A., Vooijs, M., Beverloo, H.B., Allak, B.A., van Drunen, E., Kanaar, R., Berns, A., and Jonkers, J. (2001). Growth inhibition and DNA damage induced by Cre recombinase in mammalian cells. Proc. Natl. Acad. Sci. U S A *98*, 9209–9214.

Marcu, L., Bezak, E., and Allen, B.J. (2018). Global comparison of targeted alpha vs targeted beta therapy for cancer: in vitro, in vivo and clinical trials. Crit. Rev. Oncol. Hematol. *123*, 7–20.

Nagy, A. (2000). Cre recombinase: the universal reagent for genome tailoring. Genesis *26*, 99–109.

Odagiri, H., Wang, J., and German, M.S. (1996). Function of the human insulin promoter in primary cultured islet cells. J. Biol. Chem. *271*, 1909–1915.

Pagliuca, F.W., Millman, J.R., Gurtler, M., Segel, M., Van Dervort, A., Ryu, J.H., Peterson, Q.P., Greiner, D., and Melton, D.A. (2014). Generation of functional human pancreatic beta cells in vitro. Cell *159*, 428–439.

Qasim, W., Thrasher, A.J., Buddle, J., Kinnon, C., Black, M.E., and Gaspar, H.B. (2002). T cell transduction and suicide with an enhanced mutant thymidine kinase. Gene Ther. *9*, 824–827.

Rezania, A., Bruin, J.E., Arora, P., Rubin, A., Batushansky, I., Asadi, A., O'Dwyer, S., Quiskamp, N., Mojibian, M., Albrecht, T., et al. (2014). Reversal of diabetes with insulin-producing cells derived in vitro from human pluripotent stem cells. Nat. Biotechnol. *32*, 1121–1133.

Rezania, A., Bruin, J.E., Xu, J., Narayan, K., Fox, J.K., O'Neil, J.J., and Kieffer, T.J. (2013). Enrichment of human embryonic stem cell-derived NKX6.1-expressing pancreatic progenitor cells accelerates the maturation of insulin-secreting cells in vivo. Stem Cells *31*, 2432–2442.

Russ, H.A., Parent, A.V., Ringler, J.J., Hennings, T.G., Nair, G.G., Shveygert, M., Guo, T., Puri, S., Haataja, L., Cirulli, V., et al. (2015). Controlled induction of human pancreatic progenitors produces functional beta-like cells in vitro. EMBO J. *34*, 1759–1772.

Schipper, M.L., Goris, M.L., and Gambhir, S.S. (2007). Evaluation of herpes simplex virus 1 thymidine kinase-mediated trapping of (131)I FIAU and prodrug activation of ganciclovir as a synergistic cancer radio/chemotherapy. Mol. Imaging Biol. *9*, 110–116.

Schuldiner, M., Itskovitz-Eldor, J., and Benvenisty, N. (2003). Selective ablation of human embryonic stem cells expressing a "suicide" gene. Stem Cells *21*, 257–265.

Schuldiner, M., Yanuka, O., Itskovitz-Eldor, J., Melton, D.A., and Benvenisty, N. (2000). Effects of eight growth factors on the differentiation of cells derived from human embryonic stem cells. Proc. Natl. Acad. Sci. U S A *97*, 11307–11312.

Schulz, T.C., Young, H.Y., Agulnick, A.D., Babin, M.J., Baetge, E.E., Bang, A.G., Bhoumik, A., Cepa, I., Cesario, R.M., Haakmeester, C., et al. (2012). A scalable system for production of functional pancreatic progenitors from human embryonic stem cells. PLoS One *7*, e37004.

Searle, P.F., Chen, M.J., Hu, L., Race, P.R., Lovering, A.L., Grove, J.I., Guise, C., Jaberipour, M., James, N.D., Mautner, V., et al. (2004). Nitroreductase: a prodrug-activating enzyme for cancer gene therapy. Clin. Exp. Pharmacol. Physiol. *31*, 811–816.

Tian, D., Sun, Y., Yang, Y., Lei, M., Ding, N., and Han, R. (2013). Human telomerase reverse-transcriptase promoter-controlled and herpes simplex virus thymidine kinase-armed adenoviruses for renal cell carcinoma treatment. Onco Targets Ther. *6*, 419–426.

Tsujimura, M., Kusamori, K., Oda, C., Miyazaki, A., Katsumi, H., Sakane, T., Nishikawa, M., and Yamamoto, A. (2018). Regulation of proliferation and functioning of transplanted cells by using herpes simplex virus thymidine kinase gene in mice. J. Control. Release *275*, 78–84.

Vogel, G. (2005). Cell biology. Ready or not? Human ES cells head toward the clinic. Science *308*, 1534–1538.

Williams, E.M., Little, R.F., Mowday, A.M., Rich, M.H., Chan-Hyams, J.V., Copp, J.N., Smaill, J.B., Patterson, A.V., and Ackerley, D.F. (2015). Nitroreductase gene-directed enzyme prodrug therapy: insights and advances toward clinical utility. Biochem. J. *471*, 131–153.